Available online at www.sciencedirect.com
SCIENCE DIRECT®
Journal of Solid State Chemistry 179 (2006) 2416–2425
JOURNAL OF SOLID STATE CHEMISTRY
www.elsevier.com/locate/jssc

A new anatase-type phase in the system Mg–Ta–O–N

H. Schilling[a], M. Lerch[a,*], A. Börger[b], K.-D. Becker[b], H. Wolff[c], R. Dronskowski[c], T. Bredow[d], M. Tovar[e], C. Baehtz[f]

[a]*Institut für Chemie, TU Berlin, Straße des 17. Juni 135, D-10623 Berlin, Germany*
[b]*Institut für Physikalische und Theoretische Chemie, TU Braunschweig, Hans-Sommer-Str. 10, D-38106 Braunschweig, Germany*
[c]*Institut für Anorganische Chemie, RWTH Aachen, Landoldtweg 1, D-52056 Aachen, Germany*
[d]*Theoretische Chemie, Universität Hannover, Am Kleinen Felde 30, D-30167 Hannover, Germany*
[e]*Hahn-Meitner-Institut Berlin, Glienicker Str. 100, D-14109 Berlin, Germany*
[f]*HASYLAB at DESY, Notkestr. 85, D-22603 Hamburg, Germany*

Received 13 March 2006; received in revised form 24 April 2006; accepted 27 April 2006
Available online 11 May 2006

Dedicated to Professor Hartmut Fueß on the occasion of his 65th birthday

Abstract

Magnesium doped tantalum oxynitrides were prepared by ammonolysis of amorphous mixed oxides. An orange colored anatase-type phase with the composition $Mg_{0.05}Ta_{0.95}O_{1.15}N_{0.85}$ was found. It is metastable and undergoes a phase transformation to a baddeleyite-type phase between 900 and 1000 °C. X-ray diffraction measurements indicate spacegroup $I4_1/amd$ with lattice parameters $a = 391.986(6)$ pm and $c = 1011.19(3)$ pm. A possible anion ordering was examined by theoretical methods and neutron diffraction experiments. In addition, anosovite-type (Ti_3O_5) phases $Mg_xTa_{3-x}O_{3x}N_{5-3x}$; $0 \leqslant x \leqslant 0.3$ were obtained. The electronic spectra of all phases were investigated by UV/vis spectroscopy.

Keywords: Tantalum; Oxynitrides; Ammonolysis; Baddeleyite; Anatase; Phase transformation

1. Introduction

Transition metal oxynitrides are an interesting group of materials with physical properties making them candidates for technical applications. For example, they are in the focus of recent studies testing their suitability as photocatalysts for water splitting under sunlight [1–3]. Ionic conductivity studies focusing on the behavior of N^{3-} anions have yielded promising results indicating the possibility of N^{3-} ion conducting materials [4–6]. The substitution of cadmium sulfoselenide pigments by non-toxic tantalum oxynitrides is an issue with great environmental benefits [7,8]. Transition metal oxynitrides are also materials possibly suitable as dielectrics [9,10] in microelectronic devices or as chemical gas sensors [11]. TaON and Ta_3N_5 are the basis compounds the materials in this study are derived from. TaON [12] crystallizes in the monoclinic baddeleyite-type (m-ZrO_2) structure. It can be prepared most easily by the treatment of Ta_2O_5 at ~900 °C for 16 h with flowing ammonia gas bubbled through saturated ammonia solution at a flow rate of ~20 l/h [13]. Theoretical calculations of the electronic structure of TaON gave a bandgap of 2.4 eV [14]. The olive color of TaON as it is obtained by ammonolysis is not in accord with the typical light absorption behavior of semiconductor pigments. This is probably due to a small content of reducible metal oxides in the Ta_2O_5 starting material. After a short reoxidation treatment (~800 °C) in air TaON becomes yellow [15]. Pauling's 2nd rule predicts an ordered distribution of O and N on the two anion sites that is confirmed by neutron diffraction experiments [16]. ZrO_2-like phase transitions of TaON from the monoclinic baddeleyite type to tetragonal or cubic fluorite-type phases at higher temperatures have not been detected yet. This may be explained by the relatively low decomposition

*Corresponding author. Fax: +49 30 314 79656.
E-mail address: lerch@chem.tu-berlin.de (M. Lerch).

0022-4596/$ - see front matter © 2006 Elsevier Inc. All rights reserved.
doi:10.1016/j.jssc.2006.04.036

temperature (~1100 °C) of TaON. A high pressure phase transition at ~31 GPa to the cotunnite-type structure with ninefold coordinated cations was predicted by theoretical methods [17].

Ta_3N_5 [18,19] crystallizes in the anosovite-type (Ti_3O_5) structure. It can be obtained as brick-red powder by ammonolysis of Ta_2O_5 with dry ammonia at 900 °C. Ta_3N_5 has a UV/vis absorption edge at ~600 nm corresponding to a bandgap of 2.1 eV. Absolute energies of the valence and conduction band have been determined by UPS and electrochemical measurements [20]. TEM studies [21] indicate a topotactic formation of TaON and Ta_3N_5 from Ta_2O_5.

Our study focuses on the possibilities of doping TaON and Ta_3N_5 with MgO and the resulting effects on structure and physical properties of these compounds. The preferred method for the preparation of mixed oxide precursors is the citrate route [22]. One desired effect of doping is the stabilization of new modifications of TaON. As known from ZrO_2, MgO-doping leads to the stabilization of fluorite-type structures. The stability and electronic structure of several polymorphs (baddeleyite, anatase, rutile and fluorite) of TaON has recently been studied with theoretical methods, including features like anion ordering [23]. The existence of a hexagonal α-TaON modification [24] has been falsified earlier by quantum chemical calculations [25].

2. Experimental

2.1. Synthesis

Amorphous ternary phases in the system Mg–Ta–O were prepared using a modified Pecchini method [22]. Tantalum chloride (Alfa Aesar, 99.99%) was solved in ethanol containing citric acid in an excess of 12 times the $TaCl_5$. Any dispersed Ta_2O_5 can be removed by centrifugation. The resulting tantalum citrate complexes are insensitive to water. A stock solution with a defined content of tantalum citrate has been obtained. Magnesium chloride (99.9%, Alfa Aesar) was dissolved in ethanol which contains citric acid in an excess of 12 times the $MgCl_2$. Appropriate quantities of the two citrate solutions were mixed together and ethylene glycol in an excess of 17 times the metals content was added. The solvent and HCl were evaporated and the citrate complexes together with ethylene glycol have been polymerized at ~150 °C. The organic residues of the polymer were burnt off at 600 °C for 16 h to give white X-ray amorphous powders. A series of mixed oxides $Mg_xTa_{1-x}O_{2.5-1.5x}$ with $x = 0.05$; 0.10; 0.15; 0.20; 0.25; 0.33 was prepared this way.

The amorphous mixed oxides were converted into oxynitrides by ammonolysis with either dry ammonia (3.8, Messer-Griesheim) or moist ammonia (bubbled through saturated ammonia solution) at a constant flow rate of 25 l/h at temperatures of 800 or 900 °C for 16 h.

2.2. N/O analysis

Nitrogen and oxygen contents were determined using an LECO TC-300/EF-300 N/O analyzer (hot gas extraction). Ta_2O_5 and Si_3N_4 were used as standard materials for calibration. The accuracy is ~2% of the present N/O.

2.3. Powder diffraction

A Siemens D5000 powder diffractometer (Cu$K\alpha$1 radiation, $\lambda = 154.06$ pm, position sensitive detector) was used for XRD measurements at room temperature. Temperature-dependent measurements (samples in SiO_2-glass capillaries under argon) were carried out with a STOE STADI-P powder diffractometer (Mo$K\alpha$1 radiation, $\lambda = 70.93$ pm, imaging plate detector) with a graphite heated resistance furnace. Synchrotron X-ray diffraction measurements were performed at the Hamburger Synchrotronstrahlungslabor (HASYLAB, beamline B2); neutron powder diffraction measurements at the Berlin Neutron Scattering Center (BENSC, beamline E9). The program POWDER CELL 2.4 [26] was used for quantitative phase analysis and lattice parameter determination, FULLPROF 2000 [27] for Rietveld refinements. Peak profiles were fitted with a pseudo-Voigt function.

2.4. UV/vis spectrometry

UV/vis spectra were recorded with a Perkin-Elmer Lambda 900 spectrometer equipped with a Harrick "Praying Mantis" accessory for diffuse reflection using KCl as reference. Absorbance spectra were recalculated from the measured diffuse reflectance spectra using the Kubelka–Munk formula:

$$F(R) = \frac{(1-R)^2}{2R} = \varepsilon c \frac{1}{s},$$

where R is the reflectance, ε is the absorption coefficient, c the concentration of absorbing species and s the scattering coefficient.

Bandgaps E_g were calculated using the modified Tauc equation

$$[F(R)h\nu]^{1/\beta} \sim (E_g - h\nu),$$

where $h\nu$ is the photon energy, β a coefficient depending on the nature of the optical transition (1/2 for an allowed direct transition, 2 for an allowed indirect transition).

3. Results and discussion

The anatase structure type is well known for years, but it is found in only one naturally occurring compound (TiO_2). A few synthetic materials [28–30] with anatase structure-type are known. They are formally derived from TiO_2 by anion and/or cation substitution and have titanium contents of at least 50% of the cations.

3.1. Anatase-type phase in the system Mg–Ta–O–N

Phase compositions of the ammonolysis products (moist ammonia, 800 °C) of the amorphous mixed oxides $Mg_xTa_{1-x}O_{2.5-1.5x}$; $0 \leqslant x \leqslant 0.33$ are depicted in Fig. 1. Single phase anatase-type samples of orange color were obtained at a Mg content of $x = 0.05$. An increasing fraction of rutile-type phase is formed at higher Mg contents. At $x = 1/3$, the $MgTa_2O_6$ (trirutile structure) stoichiometry is reached. The observed phase, however, possesses a simple rutile structure with randomly distributed cations.

The chemical compositions of the samples are represented graphically (Fig. 2) as lying roughly on a straight line between TaON (0 cat.-% Mg; 50 an.-% N) and $MgTa_2O_6$ (33 cat.-% Mg; 0 an.-% N) (Fig. 3) which corresponds to a 1:2 stoichiometry. The general composition on this line is $Mg_xTa_{1-x}O_{1+3x}N_{1-3x}$. Deviations of the measurements from this line may be caused by small amounts of oxygen-rich byproducts. The deviations from ideal stoichiometry could also result from crystallographic shear planes with coordination polyhedra linked by their vertices instead of their edges, which implies anion excess. Crystallographic shear planes generated by anion deficit are known e.g. from TiO_{2-x} [31] and WO_{3-x} [32]. No experimental proof for either of the hypotheses is available. Thus, the anatase-type phase should be regarded as having an ideal 1:2 stoichiometry for the time being. The composition of the anatase-type single phase is therefore given as $Mg_{0.05}Ta_{0.95}O_{1.15}N_{0.85}$. The compound can be formally understood as a solid solution of TaON and $MgTa_2O_6$:

$$Mg_{0.05}Ta_{0.95}O_{1.15}N_{0.85} = 0.85TaON.0.05MgTa_2O_6.$$

The stabilization of the anatase-type phase cannot be explained by simple arguments considering ionic radii. Mg^{2+} ($r = 72$ pm, c.n. = 6) has a higher ionic radius than Ta^{5+} ($r = 64$ pm, c.n. = 6). Incorporation of bigger cations should promote an increase of the cation coordination number. Instead of this, the coordination number of the cations changes from 7 (baddeleyite type) to 6 (anatase type). The dopant effect is possibly based on the difference

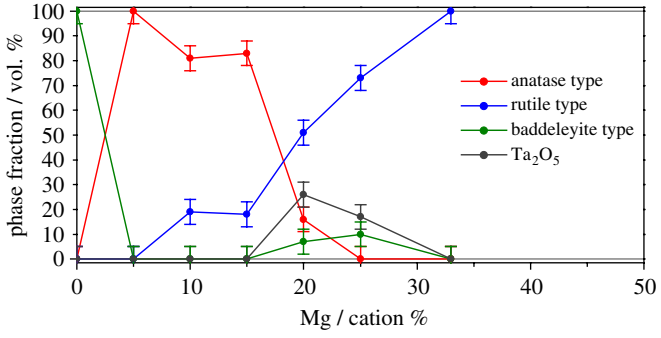

Fig. 1. Phase compositions (determined by quantitative XRD-analysis) of specimen in the system Mg–Ta–O–N obtained by ammonolysis with moist ammonia at 800 °C.

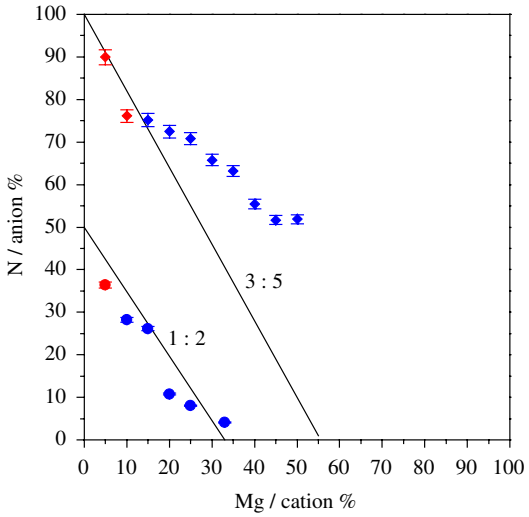

Fig. 2. Chemical compositions of the ammonolysis products obtained with moist ammonia at 800 °C (lower part) and with dry ammonia at 900 °C (upper part). Red symbols: single phase products. Lines: cation to anion ratios 1:2 and 3:5.

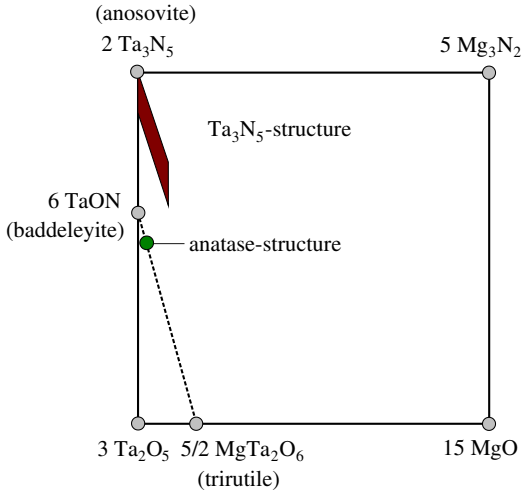

Fig. 3. Schematic representation of all new compounds obtained as single phase samples in the system Mg–Ta–O–N (colored symbols).

in the cation charge. Detailed theoretical investigations will be presented in the near future [33].

The $Mg_{0.05}Ta_{0.95}O_{1.15}N_{0.85}$ anatase-type phase was indexed in space group $I4_1/amd$ with lattice parameters $a = 391.986(6)$ pm and $c = 1011.19(3)$ pm. The c/a ratio is 2.58. From synchrotron X-ray diffraction data (Fig. 4) no deviation from the tetragonal metric was detected. The FWHMs of the X-ray reflections (synchrotron) were determined by a structureless profile fit. No anisotropic reflection broadening was found for $Mg_{0.05}Ta_{0.95}O_{1.15}N_{0.85}$.

Neutron diffraction experiments were performed with the aim to detect a possible ordering of the oxide and nitride anions on independent crystallographic sites. These anions can either be statistically distributed or located on independent crystallographic sites. The possible anion

ordering schemes have to be known prior to the evaluation of the neutron diffraction experiments. In space group $I4_1/amd$ there is only one possible anion site. Three of the *translationengleich* subgroups—$I\bar{4}m2$, $I4_1md$ and *Imma*—provide two independent anion sites [34] for the anatase structure. Each subgroup allows the anions to order in a different pattern (Fig. 5). There are only small differences between the pattern for statistically distributed anions and the ordered arrangements. The occurrence of superstructure reflections is expected for anion ordering scheme Nos. 1 and 3, but their intensity is very low. No superstructure reflections occur for anion ordering scheme No. 2. Structure model No. 3 is orthorhombic so that it may be identified by the splitting of reflections if the lattice parameter a is significantly different from b. No deviation from the tetragonal symmetry could be found from synchrotron X-ray data (Tables 1 and 2). Rietveld refinements of the neutron diffraction data show a significantly better R_{Bragg} value for $I4_1md$ compared to the other structure models (Table 3). Our complete neutron scattering work, including a detailed discussion of the anion ordering also as a function of temperature, will be presented in a forthcoming paper. Theoretical calculations on high computational level [23] gave results supporting space group $I4_1md$. These results also show that in the case of TaON, unlike TiO_2, the anatase structure is energetically favored compared to the rutile structure (Fig. 6). Calculations have been performed for anatase-type TaON (Table 4) with the three anion distributions mentioned above. The structure model in spacegroup *Imma* leads to a strong orthorhombic lattice distortion which is not detected in our X-ray diffraction measurements presented here. The calculated stability for the structure model in spacegroup $I\bar{4}m2$ is less than that of rutile-type TaON. Therefore the model in spacegroup $I4_1md$ (anion ordering scheme No. 2) is most likely the correct one. The stability

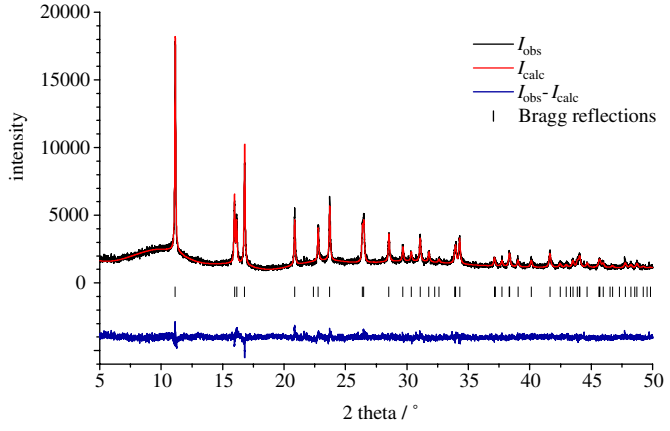

Fig. 4. X-ray powder diffraction diagram (synchrotron) of $Mg_{0.05}Ta_{0.95}O_{1.15}N_{0.85}$ with results of the Rietveld refinement in spacegroup $I4_1/amd$.

Table 1
Structural data of $Mg_{0.05}Ta_{0.95}O_{1.15}N_{0.85}$ (synchrotron radiation)

Structure type	Anatase
Formula weight	203.42 g/mol
Space group	$I4_1/amd$
Crystal system	Tetragonal
Lattice parameters	$A = 391.986(6)$ pm
	$c = 1011.19(3)$ pm
	$c/a = 2.58$
Unit cell volume	$V = 155.373(6) \times 10^6$ pm^3
Formula units	$Z = 4$
Calculated density	$= 8.71\, g/cm^3$
Diffractometer	B2/HASYLAB
Wavelength	70.990 pm
Profile points	11,249
2θ range	5–50°
Refined parameters	27
R_{wp}	6.8%
R_{Bragg}	9.0%
R_{exp}	2.4%
S	2.8

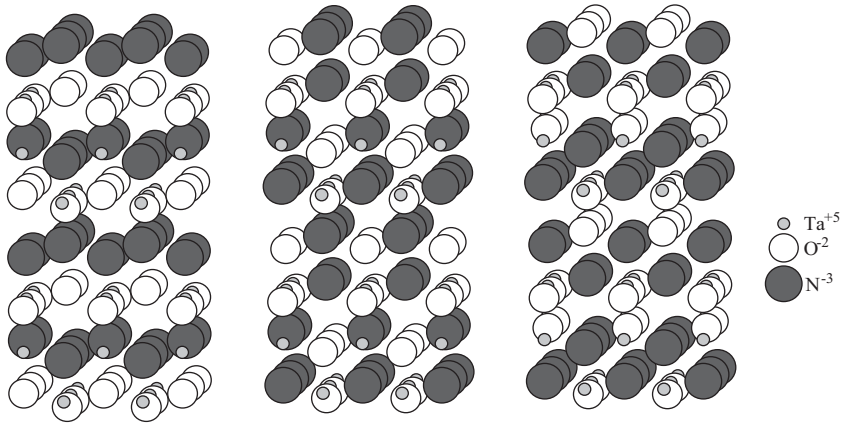

Fig. 5. Possible anion distributions for TaON in the *maximal translationengleich* subgroups of $I4_1/amd$. Left: O/N ordering pattern 1; spacegroup $I\bar{4}m2$, middle: O/N ordering pattern 2; spacegroup $I4_1md$, right: O/N ordering pattern 3; spacegroup *Imma*.

Table 2
Atomic parameters of $Mg_{0.05}Ta_{0.95}O_{1.15}N_{0.85}$ (synchrotron radiation)

Atom	Wyck.	x	y	z	Occ.	B_{iso}/Å^2
Ta/Mg	4*b*	0	1/4	3/8	0.95/0.05	0.34(3)
N/O	8*e*	0	1/4	0.584(1)	0.425/0.575	1.8(3)

Table 3
Results of the Rietveld refinements for $Mg_{0.05}Ta_{0.95}O_{1.15}N_{0.85}$ with four different anion distributions (neutron scattering)

Anion distribution		Random	No. 1	No. 2	No. 3
Space group		$I4_1/amd$	$I\bar{4}m2$	$I4_1md$	*Imma*
Crystal system		Tetragonal	Tetragonal	Tetragonal	Orthorhombic
Lattice parameters/pm	*a*	391.72(1)	391.74(2)	391.73(1)	391.7(1)
	b				391.7(1)
	c	1010.62(3)	1010.68(5)	1010.67(4)	1010.65(4)
Formula units		$Z = 4$	$Z = 4$	$Z = 4$	$Z = 4$
Diffractometer			E9/BENSC		
Wavelength			$\lambda_1 = 179.722$ pm; $\lambda_2 = 180.315$ pm; $\lambda_2/\lambda_1 = 0.05$		
Profile points			1479		
2θ range			10–160°		
Refined parameters		20	23	22	24
R_{wp}		7.57	7.90	7.54	7.69
R_{Bragg}		5.50	5.71	4.79	5.05
R_{exp}		3.78	3.78	3.78	3.78
S		2.00	2.09	1.99	2.03

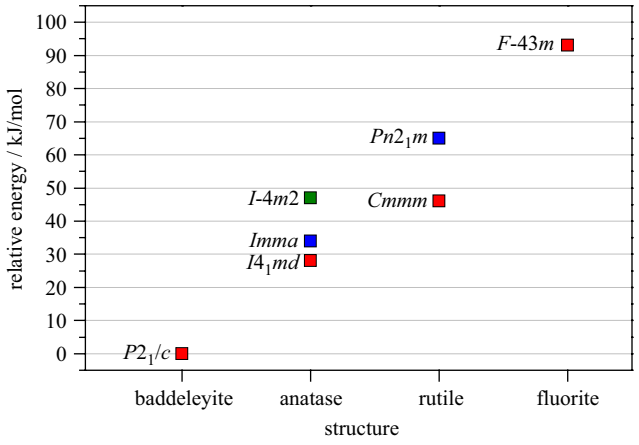

Fig. 6. Relative stabilities of possible TaON polymorphs (including different anion ordering patterns) calculated by the PW1PW method [24].

of this structure results from the anion coordination, each oxygen having six nitrogen atoms as anion neighbors and vice versa. The metastable character of the anatase-type phase has been validated by theoretical calculations. Baddeleyite-type TaON has the highest stability. The chemical composition of the compound $Mg_{0.05}Ta_{0.95}O_{1.15}N_{0.85}$ does not deviate very much from pure TaON. The results of the theoretical study should be applicable and support the results of the neutron scattering experiments. In contrast, studies on TiNF [29], also crystallizing in the anatase-type, revealed no anion ordering.

DTA/TG measurements in air have shown that at a temperature of 410 °C the oxynitride $Mg_{0.05}Ta_{0.95}O_{1.15}N_{0.85}$ reacts with oxygen to give the oxide. Under inert atmosphere (argon) a phase transformation from the anatase to the baddeleyite structure is observed (Fig. 7). The transformation proceeds gradually through a two phase domain over a temperature range from 900 to 1000 °C. The baddeleyite-type phase is preserved after cooling, evidencing an irreversible phase transformation. The anatase to rutile transformation of pure TiO_2 [35] occurs at a considerably lower temperature of ~600 °C. Although $I4_1/amd$ (anatase) is a supergroup of $P2_1/c$ (baddeleyite) [36], the observed phase transition should be considered as reconstructive because coordination polyhedra and their linking change completely. After the phase transition the substance is black, indicating a partial reduction of tantalum (V), which occurs typically under reducing atmospheres at temperatures above ~950 °C. N/O analysis, however, showed no significant loss of nitrogen. A further proof for the retention of nitrogen is given by high temperature neutron diffraction measurements of $Mg_{0.05}Ta_{0.95}O_{1.15}N_{0.85}$ (Fig. 8). A baddeleyite-type phase with the typical anion ordering known from β-TaON was found at a temperature of 1000 °C after the phase transition. Thermal expansion coefficients of $Mg_{0.05}Ta_{0.95}O_{1.15}N_{0.85}$ were determined from the neutron diffraction data (Fig. 9, Table 5 and 6): $\alpha_a = 0.31 \times 10^{-5}\,K^{-1}$ and $\alpha_c = 0.71 \times 10^{-5}\,K^{-1}$. Anatase TiO_2 possesses higher thermal expansion coefficients ($\alpha_a = 0.49 \times 10^{-5}\,K^{-1}$ and

Table 4
Results of quantum chemical calculations with the PW1PW method [24]

Anion distrib.	SG	*a*	*b*	*c*	*c*/*a*	$\Delta_a H$	BG	O coord.
A	$I\bar{4}m2$	390	—	1030	2,64	2027	2.34	2N, 4O
B	*Imma*	383	405	1003	—	2040	2.11	2O, 4N
C	$I4_1md$	392	—	1020	2,60	2046	2.85	2N, 4N
Exp. (5% Mg)	$I4_1/amd$	392	—	1010	2,58			

Lattice parameters *a*, *b*, *c* (pm), heat of atomization $\Delta_a H$ (kJ/mol), bandgap at 0 K (eV).

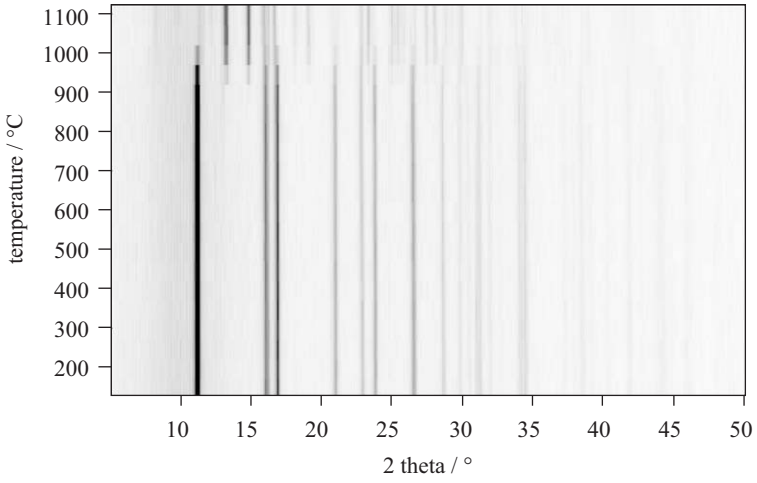

Fig. 7. X-ray powder patterns of the phase transformation of $Mg_{0.05}Ta_{0.95}O_{1.15}N_{0.85}$ from anatase to baddeleyite type occurring in the temperature range between 900 and 1000 °C under argon.

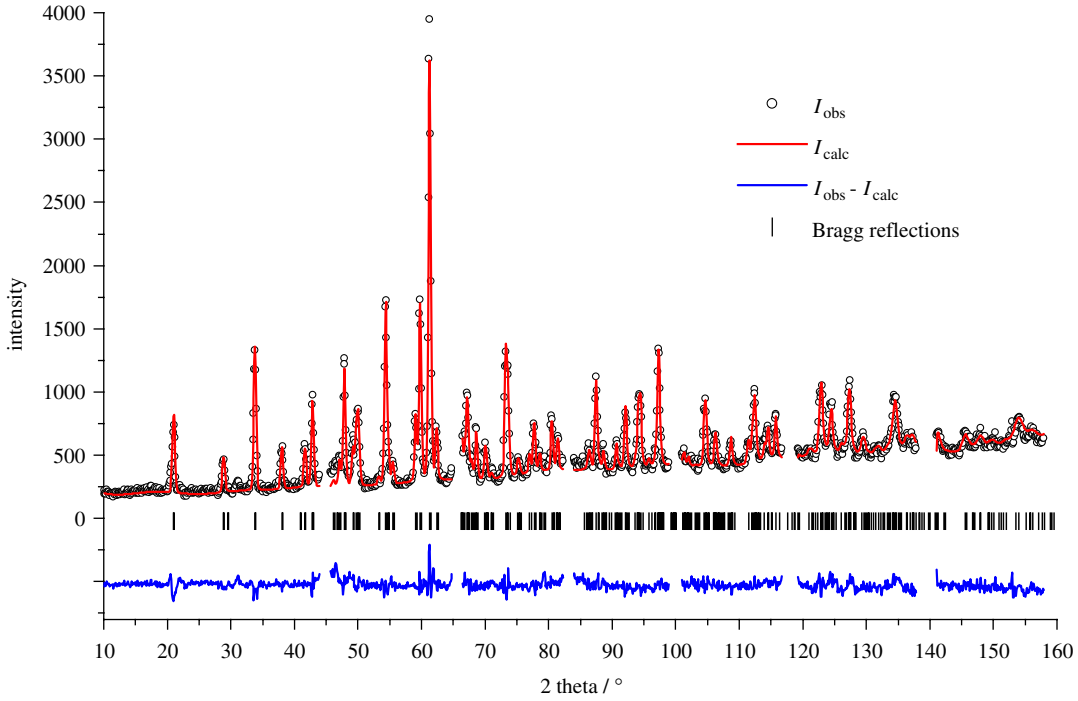

Fig. 8. Neutron powder diffraction diagram of $Mg_{0.05}Ta_{0.95}O_{1.15}N_{0.85}$ at 1000 °C after the phase transformation together with results of the Rietveld refinement (spacegroup $P2_1/c$). The reflections of the tantalum sample container are excluded.

$\alpha_c = 1.13 \times 10^{-5}\,K^{-1}$, according to our measurements). Other tantalum oxynitrides show the same trend compared with isotypic oxides. The thermal expansion of the oxynitride is always lower compared to the oxide (e.g. the volume thermal expansion coefficients γ (TaON) = $3.9 \times 10^{-5}\,K^{-1} < \gamma$ (ZrO_2) = $5.1 \times 10^{-5}\,K^{-1}$ [37]; γ (fluorite-type $Y_{0.15}Ta_{0.85}O_{0.62}N_{1.15}$) = $2.07 \times 10^{-5}\,K^{-1}$ [38] $< \gamma$ (YSZ; $Y_{0.15}Zr_{0.85}O_{1.93}$) = $3.3 \times 10^{-5}\,K^{-1}$ [39]). The volume expansion coefficient is $\gamma = 1.33 \times 10^{-5}\,K^{-1}$. Because of the different linear expansion coefficients α_a and α_c (Fig. 10), the unit cell is stretched in the *c*-direction. The *c*/*a* ratio increases from 2.58 at 25 °C to 2.59 at ~900 °C. DTA/TG measurements show neither a significant loss of mass (release of N_2) nor a DTA signal corresponding to the phase transformation. A reference experiment with TiO_2 (anatase to rutile transformation at ~600 °C, confirmed by temperature dependent XRD measurements) under air gave also no DTA signal at the transition temperature.

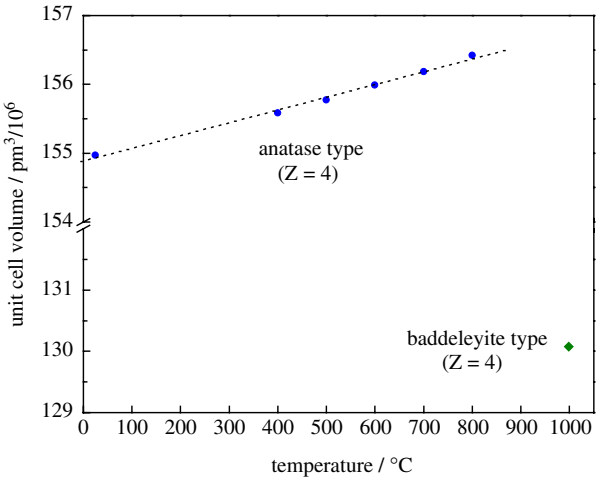

Fig. 9. Thermal volume expansion of $Mg_{0.05}Ta_{0.95}O_{1.15}N_{0.85}$ as determined from the neutron diffraction data.

Table 5
Structural data of baddeleyite-type $Mg_{0.05}Ta_{0.95}O_{1.15}N_{0.85}$ at 1000 °C from the neutron diffraction experiment

Structure type	Baddeleyite
Formula weight	203.42 g/mol
Space group	$P2_1/c$
Crystal system	Monoclinic
Lattice parameters	$a = 500.24(2)$ pm
	$b = 505.41(2)$ pm
	$c = 522.11(2)$ pm
	$\beta = 99.827(2)^\circ$
Unit cell volume	130.07×10^6 pm^3
Formula units	$Z = 4$
Diffractometer	E9/BENSC
Wavelength	$\lambda_1 = 179.722$ pm; $\lambda_2 = 180.315$ pm; $\lambda_2/\lambda_1 = 0.05$
Profile points	1351
2θ range	10–160°
Refined parameters	22
R_{wp}	7.3%
R_{Bragg}	9.8%
R_{exp}	4.5%
S	1.62

The absorption edge of anatase-type $Mg_{0.05}Ta_{0.95}O_{1.15}N_{0.85}$ has been observed at 560 nm. The bandgap is therefore 2.2 eV. The absorption at longer wavelengths drops steeply to zero, resulting in a brilliant color of the compound (Fig. 11). Despite the higher oxygen content, the absorption edge is at a substantially higher wavelength compared to β-TaON. This result, however, is no contradiction to the concept of Phillips [40], van Vechten [41] and Jorgensen [42] keeping in mind that the concept allows only a comparison between compounds with the same crystal structure. The anatase-type phases $Ti_xTa_{1-x}O_{1+x}N_{1-x}$; $0.52 \leqslant x \leqslant 0.87$ show an olive color [28]. Partial reduction of the titanium (IV) cations cannot be prevented completely under synthesis conditions. Experiments in this work

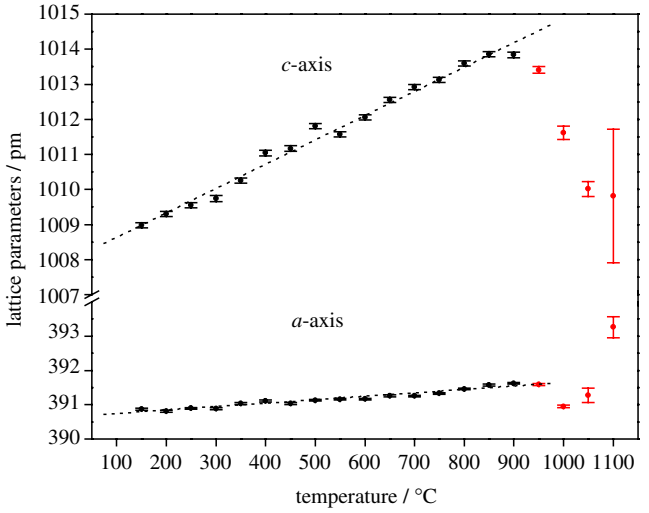

Fig. 10. Linear thermal expansion of $Mg_{0.05}Ta_{0.95}O_{1.15}N_{0.85}$ as determined from X-ray diffraction data in the temperature range 150–1100 °C. Red symbols: transformation range.

Table 6
Atomic parameters of $Mg_{0.05}Ta_{0.95}O_{1.15}N_{0.85}$ at 1000 °C from the neutron diffraction experiment

Atom	Wyckoff	x	y	z	Occ.	B_{iso}/Å^2
Ta/Mg	4*e*	0.2881(9)	0.0416(8)	0.2126(9)	0.95/0.05	1.33(8)
N/O 1	4*e*	0.4431(7)	0.7543(7)	0.4794(6)	0.85/0.15	1.44(7)
O 2	4*e*	0.061(1)	0.3281(9)	0.349(1)	1	1.43(9)

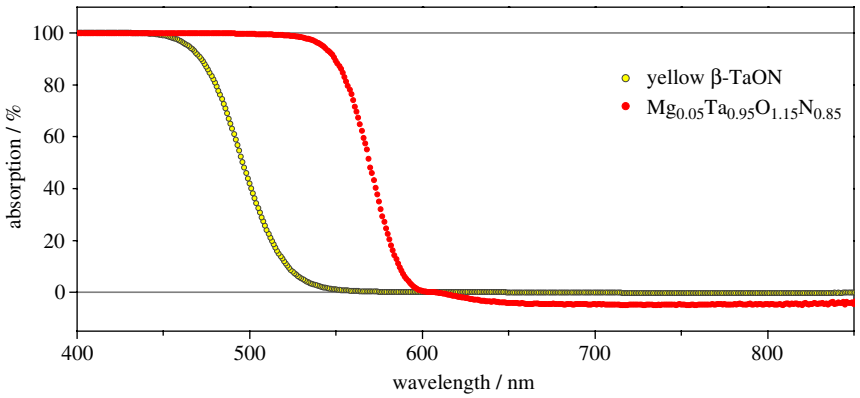

Fig. 11. UV/vis spectra of $Mg_{0.05}Ta_{0.95}O_{1.15}N_{0.85}$ and yellow β-TaON derived from diffuse reflectance measurements relative to KCl.

Table 7
Optical characteristics of Mg-doped phases with the Ta_3N_5 structure

Composition	Abs. edge (nm)	Bandgap (eV)	Step height (%)	Unit cell volume (pm^3)
Ta_3N_5	600	2.06	10	408.65×10^6
$Mg_{0.15}Ta_{2.85}O_{0.45}N_{4.55}$	595	2.08	75	407.90×10^6
$Mg_{0.3}Ta_{2.7}O_{0.9}N_{4.1}$	570	2.18	100	406.40×10^6

proved that the olive colored phases can be reoxidized by thermal treatment of some minutes at ~800 °C in air. The reoxidized compounds are of yellow color.

The pressure induced anatase to rutile phase transformation of TiO_2 is well known [43,44]. Therefore, a similar behavior of anatase-type $Mg_{0.05}Ta_{0.95}O_{1.15}N_{0.85}$ can be anticipated. For an experimental proof, samples were milled for 12 and for 48 h in an electric ball mill. The anatase-type phase disappears with increasing time of milling. X-ray reflections of a new phase, identified as baddeleyite-type, were observed. The color changes from orange to light brown. N/O analysis gives contents of 9.8 wt% O/5.6 wt% N before and 17.6 wt% O/3.0 wt% N after milling in air, indicating partial reoxidation.

Lithium ions can be intercalated into anatase-type TiO_2 with butyllithium or by electrochemical reduction [45]. The lithium intercalation causes an orthorhombic distortion (space group *Imma*) of the crystal lattice. At ~500 °C the intercalated phase changes into a spinel-type phase [46]. Some experiments have been performed in order to clarify whether $Mg_{0.05}Ta_{0.95}O_{1.15}N_{0.85}$ shows a similar behavior or not. For the lithium intercalation the samples were treated under argon atmosphere with excess butyllithium (2.5 M solution in hexane fraction). After a time of ~16 h, the samples were washed with dry *n*-hexane. They are very sensitive to moisture. The $Li_xMg_{0.05}Ta_{0.95}O_{1.15}N_{0.85}$ compound shows a brownish black color. X-ray diffraction measurements showed no orthorhombic distortion of the crystal lattice, but changes in the lattice parameters: $a = 393.38(5)$ pm and $c = 1008.2(1)$ pm. The c/a ratio changed from $c/a = 2.58$ in the educt to $c/a = 2.56$ in the intercalated phase. Temperature-dependent X-ray diffraction measurements indicate a phase transformation at ~850 °C. However, the products could not be identified due to their poor crystallinity. Li intercalation in anatase-type TaON-phases must be investigated in more detail and will be presented in a forthcoming paper.

3.2. Nitrogen-rich anosovite-type phases in the system Mg–Ta–O–N

For Mg-doped Ta_3N_5, the general composition $Mg_xTa_{3-x}O_{3x}N_{5-3x}$ can be established if a cation to anion ratio of 3:5 is maintained. An amount of up to ~10 cat.-% Mg ($0 \leqslant x \leqslant 0.3$) along with simultaneous substitution of N by O can be incorporated into the Ta_3N_5 crystal lattice. These phases were prepared by ammonolysis of amorphous mixed oxides $Mg_xTa_{1-x}O_{2.5-1.5x}$, $0 \leqslant x \leqslant 0.5$, with dry ammonia at 900 °C. The cation/anion ratio of the Mg-doped phases is ~3:5 in the composition range up to ~10 cat.-% Mg. At Mg contents above 10 cat.-% the stoichiometry deviates from 3:5 (Fig. 2), indicating these samples are Mg-'saturated' Ta_3N_5-type phases with excess MgO. The excess MgO, however, cannot be detected in the X-ray diffraction patterns. Despite the larger ionic radius of Mg^{2+} compared to Ta^{5+} the unit cell volume of the Ta_3N_5 phase is shrinking with increasing content of Mg (Table 7), supporting a structure model with anion vacancies in the anosovite-type structure. Nevertheless, this phenomenon has to be investigated in detail by computational methods [33]. UV/vis spectra of Mg doped Ta_3N_5 samples were recorded for samples with overall Mg

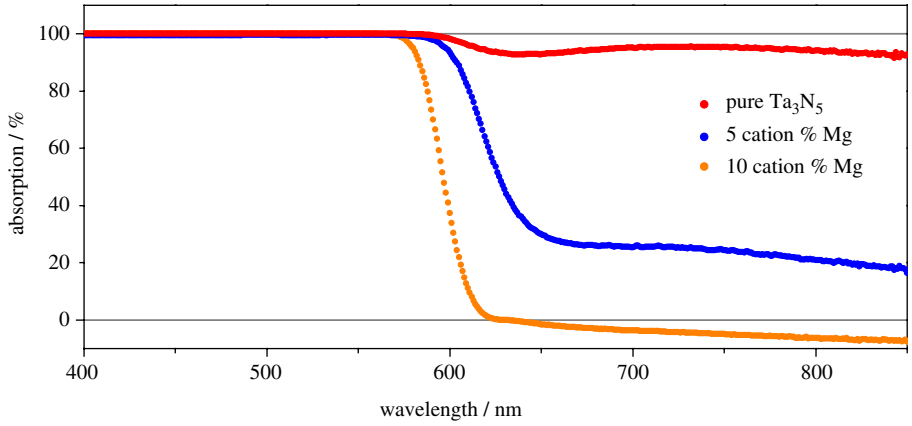

Fig. 12. UV/vis spectra of pure Ta_3N_5 and Ta_3N_5-phases with Mg contents of 5 and 10 cation %, respectively, derived from diffuse reflectance measurements relative to KCl.

concentrations of 5, 10, 15, 20 and 25 cat.-% Mg. Two different effects on the absorption characteristics were observed. Nitrogen in the anion lattice is substituted by oxygen with increasing Mg content. The absorption edge (Fig. 12) is therefore shifted towards shorter wavelengths according to the concept of Phillips [40], van Vechten [41] and Jorgensen [42]. The maximum shift was observed with 10 cation % Mg. Higher Mg contents did not increase the effect. The second effect is a decrease of the absorption at longer wavelengths from ~90% (brickred Ta_3N_5) to zero (10 cat.-% Mg). The latter sample shows a brilliant red color due to the steep increase of the absorption edge. The applicability of doped Ta_3N_5-type phases as inorganic pigments has already been demonstrated in a previous study on $Zr_xTa_{3-x}O_xN_{5-x}$, $0 \leqslant x \leqslant 0.6$ [8]. The maximum dopant content is lower for Mg than for Zr because of the greater difference in charge and ionic radius compared to the host lattice cations. The shift of the absorption edge with increasing oxygen anion content follows the same trend.

4. Conclusions

A single-phase sample with anatase-type structure ($Mg_{0.05}Ta_{0.95}O_{1.15}N_{0.85}$) was found in the system Mg–Ta–O–N. It was synthesized by ammonolysis. This is the first example of an anatase-type compound without titanium. Anion ordering patterns of *AXY* compounds in the anatase type can be described most simply in three of the *translationengleich* subgroups of $I4_1/amd$: $I\bar{4}m2$, $I4_1md$, and *Imma*—leading to three different anion ordering patterns. Rietveld refinements with neutron diffraction data of $Mg_{0.05}Ta_{0.95}O_{1.15}N_{0.85}$ and quantum chemical calculations indicate an anion ordered structure in $I4_1md$. The anatase-type phase is metastable and undergoes a phase transformation to a baddeleyite-type phase between 900 and 1000 °C. $Mg_{0.05}Ta_{0.95}O_{1.15}N_{0.85}$ shows a brilliant orange color. The absorption edge (560 nm) was determined by UV/vis spectrometry. The electronic bandgap is therefore 2.2 eV.

Ta_3N_5 can be doped with significant amounts of Mg. 10 cat.-% Mg could be incorporated into the cation sublattice along with the substitution of nitrogen by oxygen which is necessary for charge neutrality. The unit cell volume shrinks with increasing Mg content. UV/vis spectra showed a shift of the absorption edge from 600 nm (undoped Ta_3N_5) to 570 nm (10 cat.-% Mg). Samples of brilliant red color were obtained.

Acknowledgments

N/O-analysis by B. Hahn and synchrotron measurements at the HASYLAB are gratefully acknowledged. This work is supported by the DFG within the priority program 1136.

References

[1] S. Ito, K.R. Thampi, P. Comte, P. Liska, M. Grätzel, Chem. Commun. (2005) 268.
[2] M. Hara, T. Takata, J.N. Kondo, K. Domen, Catal. Today 90 (2004) 313.
[3] R. Nakamura, T. Tanaka, Y. Nakato, J. Phys. Chem. B (2005) 8920.
[4] M. Lerch, J. Lerch, R. Hock, J. Wrba, J. Solid State Chem. 128 (1997) 282.
[5] J. Wendel, M. Lerch, W. Laqua, J. Solid State Chem. 142 (1999) 163.
[6] M.A. Taylor, M. Kilo, C. Argirusis, G. Borchardt, I. Valov, C. Korte, J. Janek, T.C. Roedel, M. Lerch, Solid State Data, Part A: Defect and Diffusion Forum 479 (2005) 237–240.
[7] M. Jansen, H.P. Letschert, Nature 404 (6781) (2000) 980.
[8] E. Guenther, M. Jansen, Mater. Res. Bull. 36 (2001) 1399.
[9] J.H. Swisher, M.H. Read, Metall. Trans. 3 (1972) 489.
[10] M. Kerlau, O. Merdrignac-Conanec, M. Guilloux-Viry, A. Perrin, Solid State Sci. 6 (2004) 101.
[11] O. Merdrignac-Conanec, M. Kerlau, M. Guilloux-Viry, R. Marchand, N. Barsan, U. Weimar, Silicates Indust. 69 (2004) 141.
[12] M. Weishaupt, J. Strähle, Z. Anorg. Allg. Chem. 429 (1977) 261.
[13] S.J. Clarke, K.A. Hardstone, C.W. Michie, M.J. Rosseinsky, Chem. Mater. 14 (2002) 2664.
[14] C.M. Fang, E. Orhan, G.A. de Wijs, H.T. Hintzen, R.A. de Groot, R. Marchand, J.-Y. Saillard, G. de With, J. Mater. Chem. 11 (2001) 1248.
[15] E. Orhan, F. Tessier, R. Marchand, Solid State Sci. 4 (2002) 1071.
[16] D. Armytage, B.E.F. Fender, Acta Crystallogr. B30 (1974) 809.

[17] M.-W. Lumey, R. Dronskowski, Z. Anorg. Allg. Chem. 631 (2004) 887.
[18] G. Brauer, J.R. Weidlein, Angew. Chem. 77 (1965) 219.
[19] J. Strähle, Z. Anorg. Allg. Chem. 402 (1973) 47.
[20] W.-J. Chun, A. Ishikawa, H. Fujisawa, T. Takata, J.N. Kondo, M. Hara, M. Yasumichi, Y. Matsumoto, K. Domen, J. Phys. Chem. B 107 (2003) 1798.
[21] D. Lu, G. Hitoki, E. Katou, J.N. Kondo, M. Hara, K. Domen, Chem. Mater. 16 (2004) 1603.
[22] T. Okubo, M. Kakihana, J. Alloys Compds. 256 (1997) 151.
[23] T. Bredow, R. Dronskowski, M. Lerch, M.-W. Lumey, H. Schilling, J. Pickardt, Z. Anorg. Allg. Chem., in press.
[24] Yu.A. Buslaev, G.M. Safronov, V.I. Pachomov, M.A. Glushkova, V.P. Repko, M.M. Ershova, A.N. Zhukov, T.A. Zhdanova, Izvestiya Akademii Nauk SSSR, Neorganicheskie Materialy 5 (1969) 45.
[25] M.-W. Lumey, R. Dronskowski, Z. Anorg. Allg. Chem. 629 (2003) 2173.
[26] W. Kraus, G. Nolze, Bundesanstalt für Materialprüfung (BAM), Berlin, 2000.
[27] J. Rodriguez-Carvajal, Abstracts of the Satellite Meeting on Powder Diffraction of the XV Congress of the IUCr, 1990, p. 127.
[28] J. Grins, J. Eur. Ceram. Soc. 17 (1997) 1819.
[29] C. Wüstefeld, T. Vogt, U. Löchner, J. Strähle, H. Fueß, Angew. Chem. 100 (1988) 1013.
[30] H. Yamane, B.-C. Young, T. Hirai, J. Ceram. Soc. Japan, Int. Ed. 100 (1992) 1450.
[31] J. Booth, T. Ekstroem, E. Iguchi, R.J.D. Tilley, J. Solid State Chem. 41 (1982) 293.
[32] A.N. Cormack, C.M. Freeman, R.L. Royle, C.R.A. Catlow, Mater. Sci. Monogr. 28A (1985) 321.
[33] H. Wolff, R. Dronskowski, T. Bredow, H. Schilling, M. Lerch, in preparation.
[34] I. Sens, U. Müller, Z. Anorg. Allg. Chem. 629 (2003) 487.
[35] S.R. Yoganarasimhan, C.N.R. Rao, Trans. Faraday Soc. 58 (1961) 1579.
[36] J. Senker, H. Jacobs, M. Müller, W. Press, H. M Mayer, R.M. Ibberson, Z. Anorg. Allg. Chem. 625 (1999) 2025.
[37] O. Rahäuser, Ph.D. Thesis, Universität Würzburg, 1998.
[38] H. Schilling, H. Wolff, R. Dronskowski, M. Lerch, Fluorite-type solid solutions in the system Y–Ta–O–N: A nitrogen-rich analogue to yttria stabilized zirconia (YSZ), Z. Naturforsch. B, in press.
[39] J.W. Adams, H.H. Nakamura, R.P. Ingel, R.W. Rice, J. Am. Ceram. Soc. 68 (1985) 228.
[40] J.C. Phillips, Science 169 (1970) 1035.
[41] J.A. van Vechten, Phys. Rev. B 2 (1971) 2160.
[42] C.K. Jorgensen, Oxidation Numbers and Oxidation States, vol. 7, Springer, Berlin, 1969.
[43] Y. Suwa, M. Inagaki, S. Naka, J. Mater. Sci. 19 (1984) 1397.
[44] S. Begin-Colin, G. Le Caer, A. Mocellin, M. Zandona, Philos. Mag. Lett. 69 (1994) 1.
[45] H. Lindström, S. Södergren, A. Solbrand, H. Rensmo, J. Hjelm, A. Hagfeldt, S.-E. Lindquist, J. Phys. Chem. B 101 (1997) 7710.
[46] D.W. Murphy, M. Greenblatt, S.M. Zahurak, R.J. Cava, J.V. Wasczak, G.W. Hull Jr., R.S. Hutton, Revue de Chimie minérale 19 (1982) 441.